ZÁPADOČESKÁ UNIVERZITA V PLZNI

FAKULTA STROJNÍ

KATEDRA ENERGETICKÝCH STROJŮ A ZAŘÍZENÍ

ZÁPADOČESKÁ UNIVERZITA V PLZNI

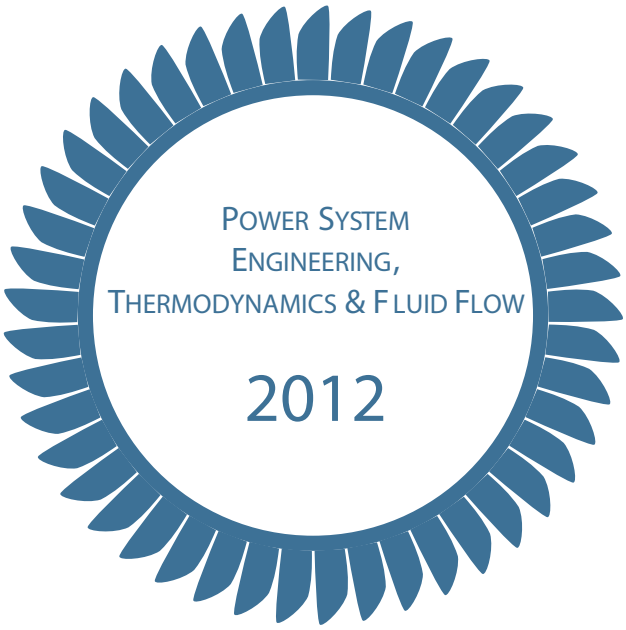


# JEDNOTLIVÝ PŘÍSPĚVEK ZE SBORNÍKU

evropský sociální fond v ČR
EVROPSKÁ UNIE
MINISTERSTVO ŠKOLSTVÍ, MLÁDEŽE A TĚLOVÝCHOVY
OP Vzdělávání pro konkurenceschopnost
INVESTICE DO ROZVOJE VZDĚLÁVÁNÍ

# NUMERICAL SOLUTIONS OF UNSTEADY FLOW IN CONVERGENT CHANNEL

**POŘÍZKOVÁ Petra, KOZEL Karel, HORÁČEK Jaromír**

*This study deals with the numerical solution of a 2D unsteady flow of a compressible viscous fluid in a channel for low inlet airflow velocity. The flow is described by the system of Navier-Stokes equations. The unsteadiness of the flow is caused by a prescribed periodic motion of a part of the channel wall, nearly closing the channel during oscillations. The channel is a simplified model of the glottal space in the human vocal tract.*

**Keywords:** CFD, FVM, unsteady flow, low Mach number, viscous compressible fluid

## Introduction

In current challenging question is a mathematical and physical description of the mechanism for transforming the airflow energy in human vocal tract (convergent channel) into the acoustic energy representing the voice source in humans.

The voice source signal travels from the glottis to the mouth, exciting the acoustic supraglottal spaces, and becomes modified by acoustic resonance properties of the vocal tract. In reality, the airflow coming from the lungs causes self-oscillations of the vocal folds, and the glottis completely closes in normal phonation regimes, generating acoustic pressure fluctuations. In this study, the periodic changes of the channel cross-section are prescribed; the channel is harmonically opening and nearly closing in the narrowest cross-section of the channel as a first approximation of reality, making the investigation of the airflow field in the glottal region possible. For phonation of vowels, the volume flow rate in the vocal tract is in the range 0.07-0.85 $l \cdot s^{-1}$ i.e. the airflow velocity in the trachea approximately in the range of 0.3-5.2 $m \cdot s^{-1}$ taking into account the tracheal diameter in humans in the range 14.5-17.6 mm [1].

Goal of this work is numerical simulation of compressible viscous flow in 2D convergent channel which involves attributes of real flow causing acoustic perturbations as is "Coandă phenomenon" (the tendency of a fluid jet to be attracted to a nearby surface), vortex convection and diffusion, jet flapping etc. along with lower call on computer time, due to later extension in 3D channel flow.

## 2. Mathematical model

To describe the unsteady laminar flow of a compressible viscous fluid in a channel, the 2D system of Navier-Stokes equations was considered as the first mathematical model. The Navier-Stokes equations were transformed to non-dimensional form. The reference dimensional variables are inflow variables (marked with the infinity subscript): the speed of sound $\underline{c}_\infty$=343 $m \cdot s^{-1}$, density $\underline{\rho}_\infty$=1.225 $kg \cdot m^{-3}$, temperature $\underline{T}_\infty$=292.75 K, dynamic viscosity $\underline{\eta}_\infty=18 \cdot 10^{-6}$ Pa·s and a reference length $\underline{L}_r$=0.02 m. The system of Navier-Stokes equations is expressed in non-dimensional conservative form [2] as:

$$W_t + F_x + G_y = \frac{1}{Re}\left(R_x + S_y\right). \tag{1}$$

$\boldsymbol{W}$ is the vector of conservative variables $\boldsymbol{W}=[\rho, \rho u, \rho v, e]^T$ where $\rho$ denotes density, $u$ and $v$ are the components of the velocity vector and $e$ is the total energy per unit volume. $\boldsymbol{F}$ and $\boldsymbol{G}$ are the vectors of inviscid fluxes and $\boldsymbol{R}$, $\boldsymbol{S}$ are the vectors of viscous fluxes. The static pressure $p$ in $\boldsymbol{F}$ and $\boldsymbol{G}$ is expressed by the state equation $p=(\kappa-1)[e-\rho/2\,(u^2+v^2)]$, where $\kappa=1.4$ is the ratio of specific heats. General Reynolds number in (1) is computed from reference variables $Re=\underline{\rho}_\infty \underline{c}_\infty \underline{L}_r / \underline{\eta}_\infty$. The non-dimensional dynamic viscosity in the dissipative terms is a function of temperature in the form $\eta=(\underline{T}/\underline{T}_\infty)^{3/4}$.

## 3. Computational domain and boundary conditions

The bounded computational domain $D$ used for the numerical solution of flow fields in the channel is shown in Fig. 1. The upper and the lower boundaries are the channel walls. A part of the walls changes its shape between the points A and B according to a given function of time and axial coordinate. The gap width (in point C) was oscillating between the minimum $g_{min}$=0.4 mm and maximum $g_{max}$=2.8 mm.

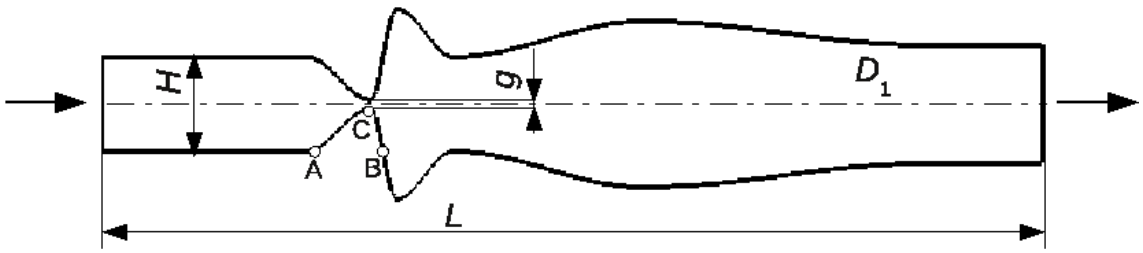


**Fig. 1:** Computational domain $D$.

The boundary conditions are considered in the following formulation:

- Upstream conditions: $u_\infty=M_\infty$, $v_\infty=0$, $\rho_\infty=1$, $p_\infty$ is extrapolated from $D$.
- Downstream conditions: $p_2 = 1/\kappa$ and $(\rho, \rho u, \rho v)$ are extrapolated from $D$.
- Flow on the wall: $(u, v) = (u_{wall}, v_{wall})$ and $\partial T/\partial \boldsymbol{n}=0$ $(T=\kappa p/\rho)$.

The general Reynolds number in (1) is multiply with non-dimensional value $H\,M_\infty$ represents kinematic viscosity scale and for computation of the real problem inlet Reynolds number $Re_\infty=\underline{\rho}_\infty \underline{c}_\infty M_\infty \underline{L}_r H/\underline{\eta}_\infty$ is used.

## 4. Numerical solution

The numerical solution uses finite volume method (FVM) in cell centred form on the grid of quadrilateral cells. In the time-changing domain, the integral form of FVM is derived using the ALE formulation. The ALE method defines homomorphic mapping of the reference domain $D_{t=0}$ at initial time $t$=0 to a domain $D_t$ at $t > 0$ [3].

The explicit predictor-corrector MacCormack (MC) scheme in the domain with a moving grid of quadrilateral cells is used. The scheme is the 2nd order accurate in time and space [4].

To stabilize computation the Jameson artificial dissipation is added to the MC scheme [5]. Since the artificial dissipation term is of third order, the overall accuracy of the scheme is of second order.

The grid used in the channel has successive refinement cells near the wall see Fig. 2. The minimum cell size in *y*-direction is $\Delta y_{min} \approx 1/\mathrm{Re}^{1/2}$ to capture the boundary layer effects.

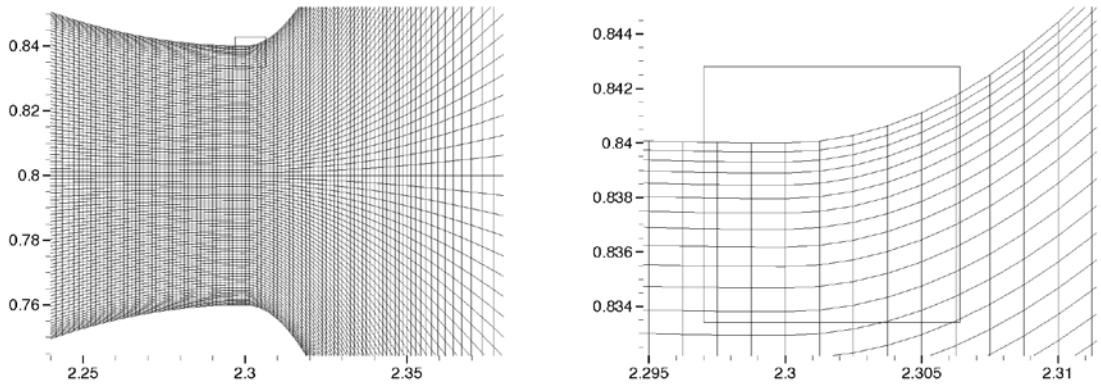


**Fig. 2:** Grid of quadrilateral cells in narrowest part of domain *D* at the middle position of the gap width - detail. $\Delta y_{min}$ = 0.0005 (0.01 mm).

## 3. Numerical results

The steady numerical results were obtained (using a specifically developed program) for the following input data:

A) *Uniform inflow* Mach number $M_\infty$=0.012 ($\underline{u}_\infty$=4.116 m·s$^{-1}$) at the inlet, atmospheric pressure $p_2$=1/κ (102942 Pa) at the outlet, Reynolds number $\mathrm{Re}_\infty$=4481 and furthermore for unsteady simulation the wall oscillation frequency was $f$=100 Hz. The computational domain contained 450 x 100 cells in *D*.

B) *Parabolic profile* of inflow Mach number $M_\infty$=0.012 at the inlet, atmospheric pressure $p_2$=1/κ at the outlet, Reynolds number $\mathrm{Re}_\infty$=4481. The computational domain contained 450 x 100 cells in *D*. The parabolic profile was pre-computed in rectangular channel (*H* x *L*) with input data as in case A).

The computation is carried out in two stages. First, a steady numerical solution is obtained, when the channel between points A and B has a rigid wall fixed in the middle position of the gap width. It is also called initial condition. This initial condition is used for the non-stationary simulation (see [6]).

Fig. 3 shows the steady numerical solutions for *uniform inflow* input data (A) and *parabolic profile* input data (B). The maximum Mach number computed in domain was $M_{max}$=0.177 (60.7 m·s$^{-1}$) in case (A) and $M_{max}$=0.162 (55.6 m·s$^{-1}$) in case (B). The pictures display non-symmetric flow developed behind the narrowest channel cross-section. Fig. 4 shows the convergences to the steady state solution computed using the $L_2$ norm of momentum residuals ($\rho u$) for both cases. The graphs indicate the non-stationary solution of initial condition which is caused probably by eddies separated in the un-movable glottal orifice and floating away.

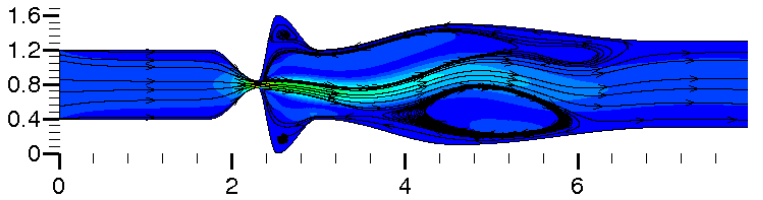


(A) $M_{max}$=0.177 (60.7 m·s$^{-1}$)

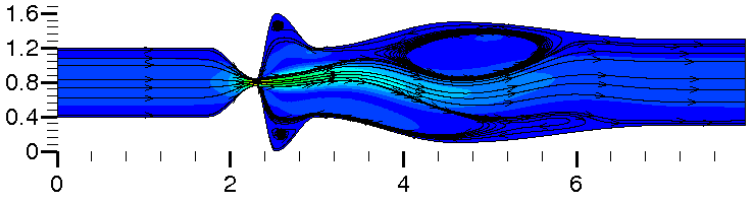


(B) $M_{max}$=0.162 (55.6 m·s$^{-1}$)

**Fig. 3:** The steady numerical solutions for *uniform inflow* input data (A) and *parabolic profile* input data (B). Mesh 450 x 100 cells in *D*.

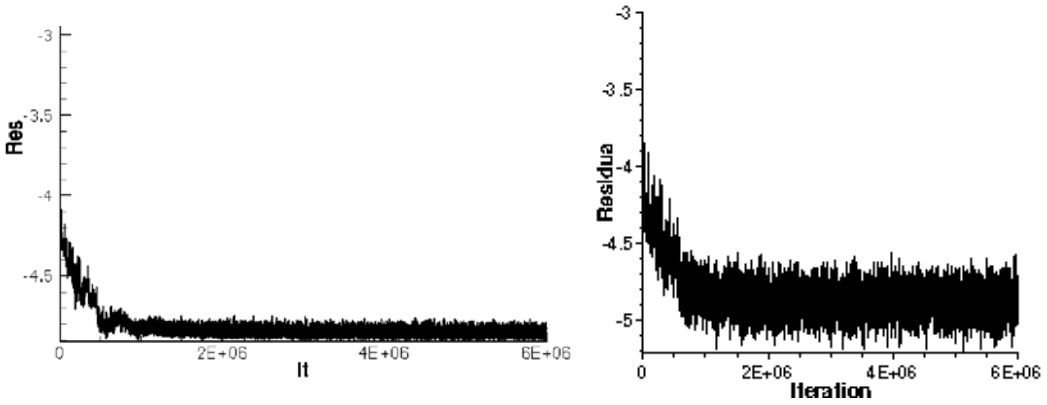


(A) (B)

**Fig. 4:** The convergence to the steady state solution for *uniform inflow* input data (A) and *parabolic profile* input data (B). Mesh 450 x 100 cells in *D*.

The non-stationary numerical simulation for *uniform inflow* input data computed in domain *D* with wall oscillation frequency *f*=100 Hz over the fifth cycle of the wall oscillation is presented in Fig. 5 showing the flow field in five time instants during one vibration period. Large eddies are developing in supraglottal spaces and the "Coandă effect" is apparent in the flow field pattern. The absolute maximum of Mach number $M_{max}$=0.535 (183.5 m·s$^{-1}$) in the flow field during period was achieved at time *t*=44.18 ms (*g*=1.0019 mm, opening phase) behind the narrowest channel cross-section. The mathematical model (1) of laminar flow used in the computation is debatable. For the first approximation, we supposed unformed turbulent flow at the inlet part of the channel.

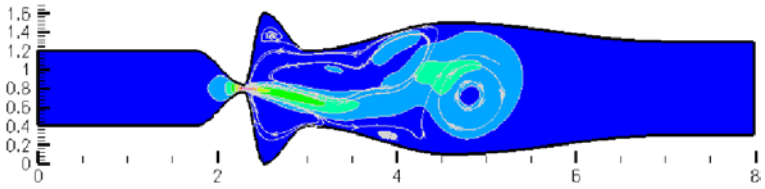

(a) $t$=40 ms, $M_{max}$=0.159 (54.8 m·s$^{-1}$)

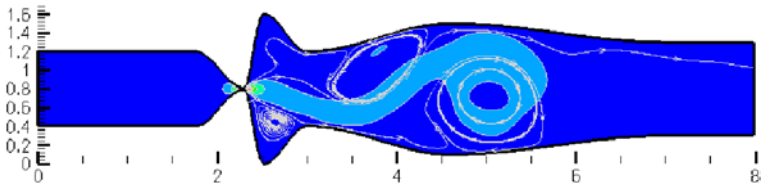

(b) $t$=42.5 ms, $M_{max}$=0.236 (80.9 m·s$^{-1}$)

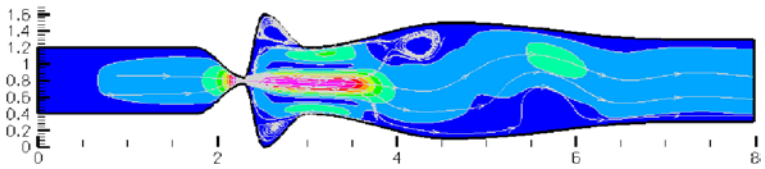

(c) $t$=45 ms, $M_{max}$=0.370 (126 m·s$^{-1}$)

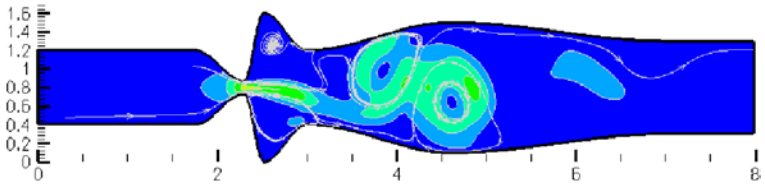

(d) $t$=47.5 ms, $M_{max}$=0.097 (33.3 m·s$^{-1}$)

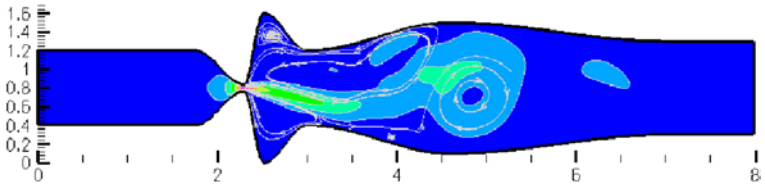

(e) $t$=50 ms, $M_{max}$=0.160 (54.9 m·s$^{-1}$)

**Fig. 5:** The non-stationary numerical simulation for *uniform inflow* input data computed in domain *D* with wall oscillation frequency $f$=100 Hz over the fifth cycle of the wall oscillation. Mesh 450 x 100 cells in *D*.

## Conclusion

The steady numerical results showed in Fig. 3 have similar flow field patterns but direction of the jet behind the gap is in opposite. Redirection of the jet was observed e.g. in [7], the jet direction is changing along with mesh configuration, modification of computational loop and channel prolongation at the inlet and outlet part of the channel. Maximal velocity in case A (*uniform inflow*) is larger by 9.25% than in case B (*parabolic profile*). The jet direction developed in the flow field of initial condition is appearing in non-stationary numerical simulation as shown in Fig. 4 (a, b, d, e) for case A (*uniform inflow*).

The numerical solution in the channel showed large vortex structures developed in the supraglottal space moving slowly downstream and decaying gradually. It was possible to detect the "Coandă phenomenon" in the computed flow field patterns. A similar generation of large-scale vortices, vortex convection and diffusion, jet flapping, and general flow patterns were experimentally obtained in physical models of the vocal folds by using PIV (Particle Image Velocimetry) method in [8].

## Reference

[1] TITZE, I.R. Principles of Voice Production. National Centre for Voice and Speech, Iowa City, 2000. ISBN 0-87414-122-2.

[2] FÜRST, J.; JANDA, M.; KOZEL, K. Finite volume solution of 2D and 3D Euler and Navier-Stokes equations. In: P. Neustupa, J. Penel (Eds.), Mathematical fluid mechanics, 173-194, Berlin, 2001.

[3] HONZÁTKO, R.; HORÁČEK, J.; KOZEL, K. Solution of inviscid incompressible flow over a vibrating profile. In: M. Beneš, M. Kimura, T. Nataki (Eds.), COE Lecture notes, **3**: 26-32, Kyushu university, 2006. ISSN 1881-4042.

[4] POŘÍZKOVÁ, P.; KOZEL, K.; HORÁČEK, J. Numerical Comparison of Unsteady Compressible Viscous Flow in Convergent Channel. In: Proceedings of the International Conference Applications of Mathematics 2012. Praha: Matematický ústav AV ČR, 2012, p. 203-213. ISBN 978-80-85823-60-8.

[5] JAMESON, A.; SCHMIDT, W.; TURKEL, E. Numerical solution of the Euler equations by the finite volume methods using Runge-Kutta time-stepping schemes, AIAA,81-125,1981.

[6] HORÁČEK, J.; ŠIDLOF, P.; URUBA, V.; VESELÝ, J.; RADOLF, V.; BULA, V. PIV Measurement of Flow-Patterns in Human Vocal Tract Model. In: Proceedings of the International Conference on Acoustic NAG/DAGA 2009, 1737-1740, Rotterdam, 2009.

[7] POŘÍZKOVÁ, P.; KOZEL, K.; HORÁČEK, J. Numerical tests of flow in human vocal tract. In: Interaction of Dynamic Systems with Surroundings and Systems with Feedbacks. Prague: Institute of Thermomechanics, AS CR, v.v.i., 2010, p. 79-86. ISBN 978-80-87012-29-1.

## Acknowledgement

This contribution was partially supported by Research Plan MSM 6840770010 and by the grants of the GA CR No. 201/08/0012 and P101/11/0207.

Ing. POŘÍZKOVÁ Petra, Ph.D., Institute of Thermomechanics AS CR, Dolejškova 5, Prague 8, Czech Republic, puncocha@marian.fsik.cvut.cz.
Prof. RNDr. KOZEL Karel, DrSc., Czech Technical University in Prague, Faculty of Mechanical Engineering, Department of Technical Mathematics, Karlovo náměstí 13, Prague 2, 121 35, Czech Republic, Karel.Kozel@fs.cvut.cz..
Ing. HORÁČEK Jaromír, DrSc., Institute of Thermomechanics AS CR, Dolejškova 5, Prague 8, Czech Republic, jaromirh@it.cas.cz.